VIRUS characterization development and results from first batches of delivered units

Indahl, Briana, Hill, Gary, Drory, Niv, Gebhardt, Karl, Tuttle, Sarah, et al.

Briana L. Indahl, Gary J. Hill, Niv Drory, Karl Gebhardt, Sarah Tuttle, Jason Ramsey, Greg Ziemann, Taylor Chonis, Trent Peterson, Andrew Peterson, Brian L. Vattiat, Huan Li, Lei Hao, "VIRUS characterization development and results from first batches of delivered units," Proc. SPIE 9908, Ground-based and Airborne Instrumentation for Astronomy VI, 990880 (9 August 2016); doi: 10.1117/12.2231915

Event: SPIE Astronomical Telescopes + Instrumentation, 2016, Edinburgh, United Kingdom

VIRUS Characterization Development and Results from First Batches of Delivered Units

Briana L. Indahl[a], Gary J. Hill[a,b], Niv Drory[b], Karl Gebhart[a], Sarah Tuttle[b], Jason Ramsey[b], Greg Ziemann[a], Taylor Chonis[a], Trent Peterson[b], Andrew Peterson[b], Brian L. Vattiat[b], Huan Li[c], and Lei Hao[c]

[a]Department of Astronomy, University of Texas at Austin, 2515 Speedway Drive, Austin, TX, USA
[b]McDonald Observatory, University of Texas at Austin, 2515 Speedway Drive, Austin, TX, USA
[b]Shanghai Astronomical Observatory

ABSTRACT

The Visible Integral Field Replicable Unit Spectrograph (VIRUS), the instrument for the Hobby Eberly Telescope Dark Energy Experiment (HETDEX), consists of 78 replicable units, each with two integral field spectrographs. Each spectrograph has its own 2kx2k CCD detector with 15 micron pixels. Following alignment, the final stage prior to deployment of each unit is characterization of the 156 spectrograph channels and their CCDs. We describe the laboratory calibration system and scripting that automates this process. Both fiber and continuous (non-spatially modulated) input slits are utilized. Photon transfer curves are made to measure the gain and read noise of each CCD. Pixel flats are also made to correct for pixel-to-pixel QE variations. Relative throughput measurements of each unit are made using the same lab fiber bundle for consistency, and fiber profiles are characterized for later use by the CURE data reduction package. Replicable unit instruments provide a cost effective solution for scaling up instruments for large and extremely large class telescopes. Because VIRUS is the first massively replicated instrument, we have the opportunity to examine the end result of variations in the manufacturing processes that go into production. This paper presents the characterization setup for VIRUS units and compares the performance and variability of processed units with specifications for HETDEX.

Keywords: CCD, detectors, characterization, Spectrographs: Integral Field, Spectrographs: VIRUS, Spectrographs: performance, Telescopes: Hobby-Eberly

1. INTRODUCTION

The Hobby Eberly Telescope Dark Energy Experiment (HETDEX) aims to survey nearly 0.8 million Lyman-emitting galaxies from $2.9 > z > 3.5$ to be used as tracers of large scale structure in the universe. In order to survey emission-line objects in the targeted 420 square degree patch of the sky, wide-field integral field spectroscopy is required. To conduct this massive survey, a revolutionary new multiplexed instrument, Visible Integral-Field Replicable Unit Spectrograph (VIRUS), is currently being constructed for the 9.2 meter Hobby Eberly Telescope (HET) at McDonald Observatory in West Texas. The instrument design takes advantage of large scale replication of simple units to significantly reduce engineering and production costs of building a facility instrument of this scale for a large telescope.

VIRUS consists of 78 replicable units, each with two integral field spectrographs. A single unit is fed a dense pack fiber bundle containing 448, 266μm (1.5 arcseconds on sky) fibers arrayed on a 50x50 $arcsec^2$ sky area with a 1/3 fill factor. Each spectrograph is then fed 224 fibers through a collimator slit. the collimator housing is shared between the two spectrographs with a baffle separating the channels. Through a volume phase holographic (VPH) gratings light enters the aluminum cast vacuum cryostat housing the two Schmidt design

Further author information: (Send correspondence to B.L.I.)
B.L.I.: E-mail: blindahl@astro.as.utexas.edu, Telephone: 1 414 232 3958
G.J.H.: E-mail: hill@astro.as.utexas.edu, Telephone: 1 414 471 1477

Ground-based and Airborne Instrumentation for Astronomy VI, edited by Christopher J. Evans, Luc Simard, Hideki Takami
Proc. of SPIE Vol. 9908, 990880 · © 2016 SPIE · CCC code: 0277-786X/16/$18 · doi: 10.1117/12.2231915

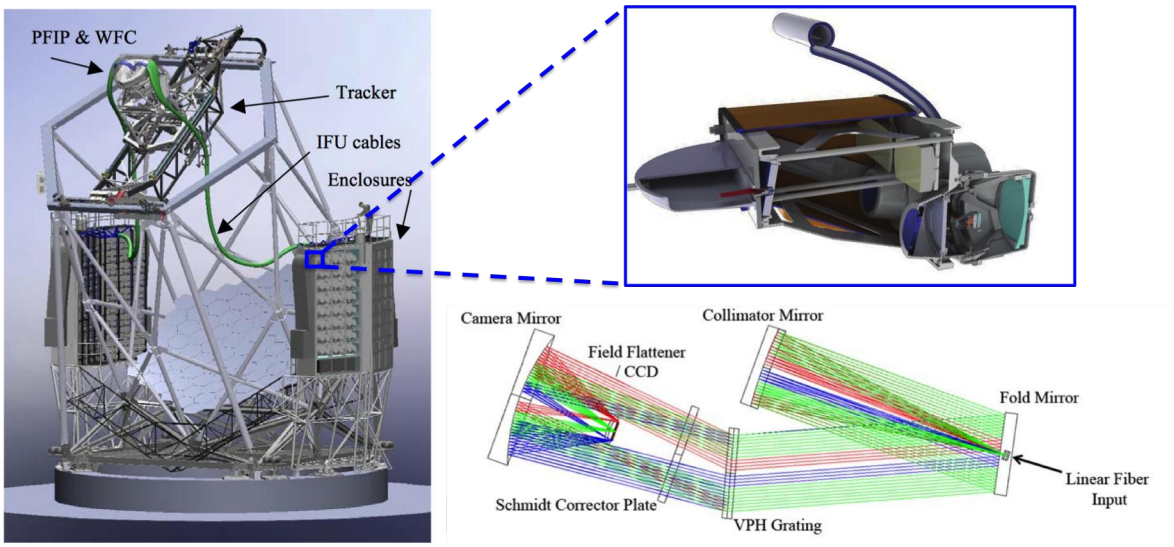

Figure 1. On the left is a drawing of the HET with the VIRUS enclosures on both sides. Each enclosure houses 40 units. A zoom a schematic of a single VIRUS unit is shown on the upper right with its optical layout underneath.[1]

cameras. The entire spectrograph consists of just 3 reflective and 2 refractive optics with an dielectric reflective coatings to optimize throughput. VIRUS covers a spectral range of 350-550nm at R 700.[1,2] 78 fiber bundles observe the newly upgraded HET's 22 arcmin focal plane[3,4] with a 1/4.5 fill factor. In a single observation with VIRUS, 156 spectrographs image nearly 35,000 spectra.[1,2]

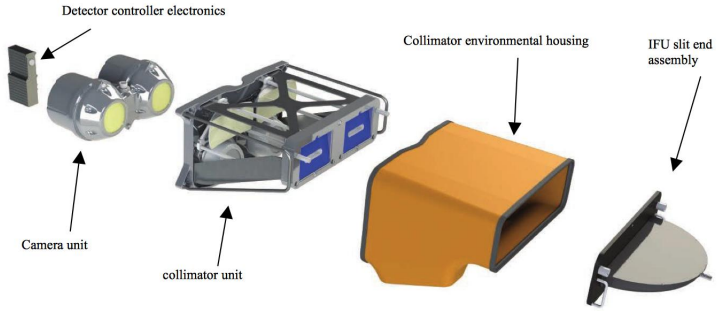

Figure 2. This image is an exploded view of a VIRUS unit highlighting its main components. Starting from the right is the IFU slit assembly which fans out the 448 fibers in the bundle along 2 slits. This feeds light to the back of the collimator covered in a housing to shroud it from stray light. The collimator attaches to the cryostat camera with its paired detector controller shown on the far left.[1]

The VIRUS concept was tested with the Mitchell Spectrograph, or the VIRUS-Prototype. A pilot survey of Lyman-α emitting galaxies proved the design, throughput, and sensitivity of the VIRUS concept for HETDEX.[5] The Mitchell Spectrograph now remains a facility instrument on the 2.7 m Harlan J. Smith Telescope at McDonald Observatory and has been used for studies of high redshift and local resolved galaxies.[6]

This type of massive replication will become a cost effective way to built monolithic instruments for the upcoming class of extremely large telescopes. With VIRUS being the first largely replicable instrument we have the chance to uncover the statistical variations in production of these units. This paper discuses the development of VIRUS characterization to test the performance in lab of each unit and the results for the first batch deployed.

Each VIRUS unit progresses through and assembly line of stages before deployment. Each unit starts with assembly of the optical and detector systems which are then mounted into the cryostat. Each one of these camera units is paired with a collimator and moves on to alignment where both a camera an collimator mirror

are adjusted for focus and image quality.[7] This paper discusses the final stage of characterization of the detector system of each aligned spectrograph before deployment. Section 2 provides an overview of the detector system and vendor specifications. Section 3 explains the lab setup in which characterization data is taken. This includes discussion of the lab calibration unit (LCU) which provides the light sources and software used to interact with both the the LCU and the the detector system. Section 4 outlines the data taking scripts written to coordinate two separate hardware systems and to automate the data taking process for characterization along with the data included in the set. Section 5 explains the analysis procedures for characterization and results of this analysis. Deployment of the first batch of units is discussed in 6. The final section 7 summarizes this work.

2. DETECTOR SYSTEM

Each spectrograph contains a 2064x2064 format CCDs with 15μm pixels and 100% fill factor. The University of Arizona Imaging Technology Laboratory is providing thinned backside illuminated CCDs from wafers manufactured by Semiconductor Technology Associates, Inc.[8] The CCDs are thinned and backside illuminated to enhance the response of the blue. AR coatings optimize the CCDs for the VIRUS bandpass. Each CCD is equipped with 4 readout amplifiers. Two are used for readout at a time and can be switched via a jumper in the flex cable. The CCDs are capable of user selected binning. HETDEX observations will be taken with 2x1 (columns x rows) binning to shorten detector readout to about 20 seconds. The entire VIRUS system is about 630 Mpixels. An observation of one HETDEX field requires 20 minute exposures for 3 dithers. With parallel readout of the 156 detectors, 2.5 GB of data are produced per observation.

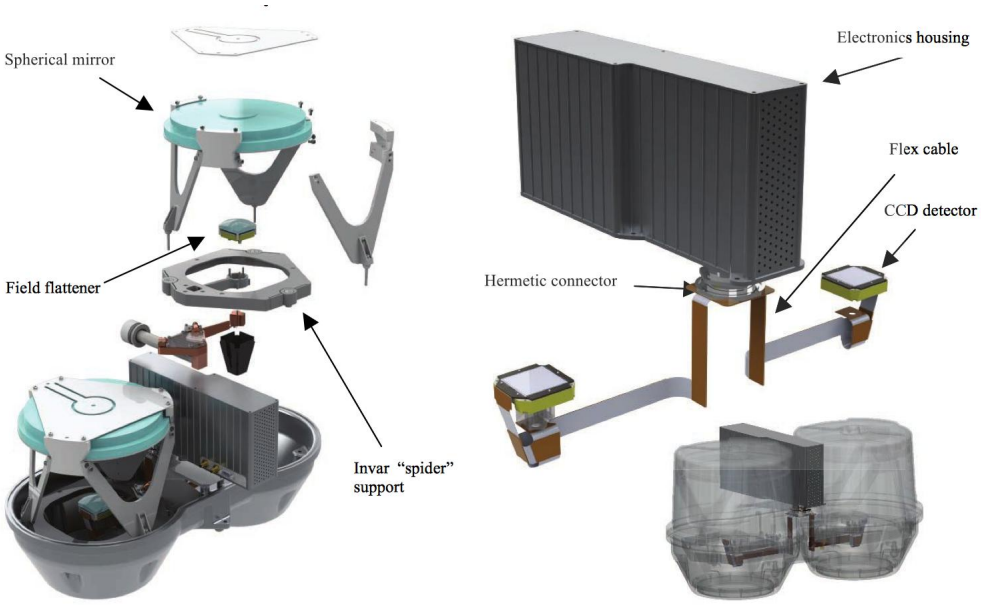

Figure 3. The left image shows an exploded schematic of the inside of the camera cryostat as discussed in Sec. 2. The upper right image show the detector system and its connections to the controller via flex cable.[1]

The detectors are housed inside the camera cryostat composed of two aluminum castings. This cryostat vacuum is shared between two units significantly reducing the number of seal surfaces, increasing the vacuum lifetime.[1] Refer to Ref. 9 for details of the cryogenic system. To ensure temperature stability, as is crucial to reach science goals for HETDEX, the detector spider mount are cast from Invar and an Invar truss supports the camera mirror. Four Invar clips mount the fused silica field flattener (FF) lens on top of the CCD. A cold block mounted to the back of the CCD controls its temperature through its connection to the cold finger and resistive heating elements. The CCD attaches to an arm protruding into the center of the spider mount. The spider design, is optimized to minimize obstruction of light to the primary spherical mirror. A flex cable interfaces the CCD and the cold block heater and temperature censor with a central bulkhead connector shared between both channels of the unit. This cable lies flush with the spider arm to prevent further obstruction. CCD controllers

connect through the bulkhead connector controlling the two detectors inside the unit. Refer to figure 3 for a detailed schematic of a VIRUS camera.[7]

2.1 Detector specifications

In order to increase detector yield and save on cost, specification metrics are applied to batches of detectors in order to reach an average performance required for HETDEX science goals. For example the quantum efficiency (QE) of a signal detector at 400 nm needed to exceed a minimum value of 70%, while the average performance of the entire batch needed to exceed 88%. A plot of QE of the delivered detectors shows they exceeded this specification especially for the redder wavelengths as shown in figure 4.[7] Other CCD specifications include the following,

1. Read noise must not exceed 4.2 e- for any batch of CCDs for any binning mode[7]
2. Fewer than 0.2% of the pixels on each CCD chip can be non-functional.
3. CCD dark count shall be less than 1 electron per pixel within a 600 second integration time.
4. The combined response of the CCD and controller shall be linear to $\geq \pm 1\%$ over the entire 16-bit dynamic range
5. Both serial and parallel Charge Transfer Efficiency (CTE) per pixel shall be better than 0.99999.[8]

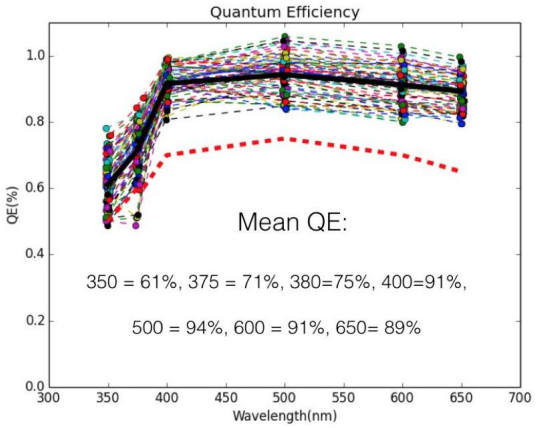

Figure 4. This is a plot of the quantum efficiency of the delivered detectors measured from the vendor.[7]

3. LAB SETUP

A separate lab at UT Austin is dedicated to detector characterization. The detectors are characterized inside their respective units with their paired controller. A light tight room inside this lab houses a cryogenic system for cooling a single unit before and during characterization. The detectors or kept at -110 Celsius during data taking, the operating temperature they will be at on the HET. The hardware computer for data taking and the mux sit outside this room to shield the unit from the mux LEDs or screen light. As a final precaution the unit is also covered in a thick black shroud to further guard against any stray light. The next subsections describe three separate systems that provide light sources and shuttering, feed light to the unit, and a brief discussion of the software controlling exposures of the detector.

3.1 Feeds

On the HET the spectrograph units are feed light through their paired fiber bundle. VIRUS units are not paired with their respective fiber bundles until deployment to the HET. Each unit in the lab is characterized with the same fiber bundle to properly characterize the detector system without including variance of fiber bundle throughput. To choose the bundle used for characterization, six were tested in lab with a single unit. A production fiber bundle with the best contrast and focus was chosen. There are two data taking modes for characterization. The spectrograph unit can either be coupled with the fiber bundle or the pixel flat head to

image a flat field of the detector. On the pixel flat head, a large glass plate replaces the fiber slit assembly where the fibers would lay across the entrance slits. light is fed through the plate with a liquid light guide. The glass plate subsequently scatters light across the slits allowing it to enter the spectrograph as a continuous source.

3.2 Lab Calibration Unit (LCU)

For characterization, both emission and continuum sources are fed to to the spectrograph from the Lab Calibration Unit (LCU) as shown in Fig. 5. The LCU was designed and built by Taylor Chonis to replace the Facility Calibration Unit (FCU) that was taken to the HET for VIRUS calibration on the telescope.

The Laser Driven Light Source (LDLS) (Energetiq EQ-99XFC) provides a very uniform and stable source of light across the spectral range of VIRUS and beyond. Each CCD is characterized within its respective spectrograph unit meaning light fed through the instrument passes through the transmission grating so the uniformity of this source from 350 to 550 nm is essential for continuous and fiber flat fielding of the chips. Mercury (Newport 6034 or 6035) and Cadmium (UVP 90-0071-03) Penray lamps provide the emission line sources for wavelength calibration.

Light from the Penray emission sources are scattered in a reflective aluminum box essentially acting as a integrating sphere. It is then fed through a compound parabolic concentrator (CPC) that couples to the liquid light guide output. The continuum source from the LDLS is fed into the same box through 230 micron fiber optic cable. LDLS light exits this cable and enters the CPC collimated along its axis. This design optimises throughput of the sources while avoiding moving mechanical parts. For taking flats with the LDLS, the output liquid light guide can be connected directly to the pixel flat head. Fibers are coupled to the output liquid light guide through the IFU Illuminator Assembly. Optimizing LDLS output was a priority for taking flat field images since the pixel flat head inherently has low throughput. The LCU includes the ability to insert a 4.0 OD neutral density filter for when the much higher throughput fibers are coupled to the system to avoid saturating fiber images.

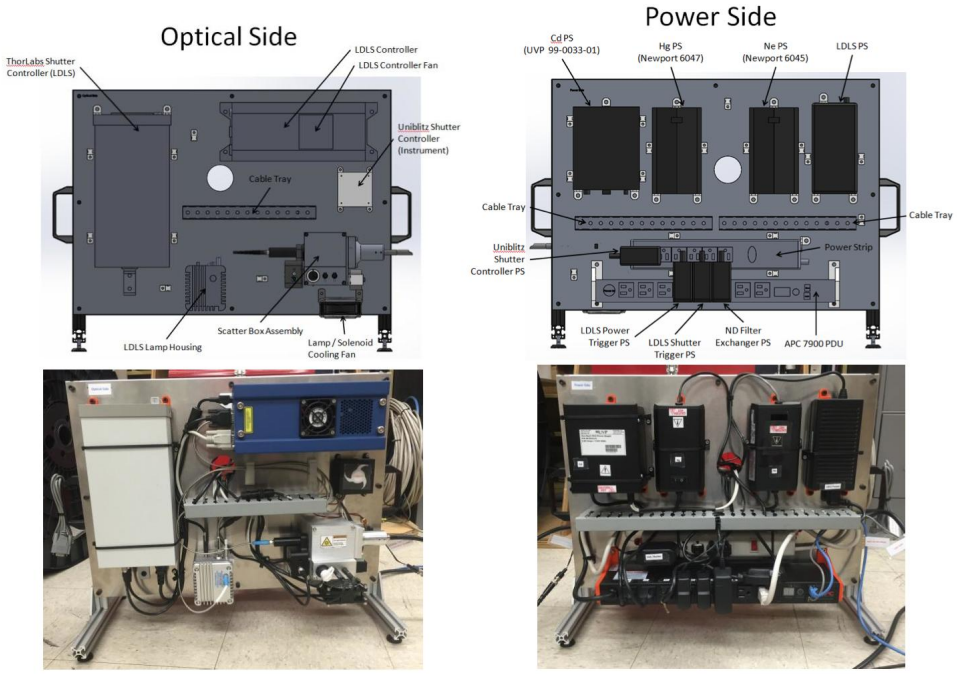

Figure 5. This figure shows a detailed schematic of the LCU. This schematic comes from Ref.[10] where a more detailed discussion of all of its components can be found.

The system contains two shutters. A Uniblitz shutter sits between the neutral density filter and the CPC and acts as the instrument shutter and is controlled by the CAMRA server's expose command. The second shutter from Thorlabs acts to shutter the LDLS. It sits right after the LDLS fiber output. This prevents frequent turning

on and off of the LDLS, preserving its limited lifetime. Chonis wrote a set of python functions to interact with the hardware. This made it possible for LCU controls to be scripted to work in series with instrument commands.[10]

3.3 CAMRA software

The CCD Array Management and Recording Application (CAMRA) provides configurable temperature, bias offset, readout, and shutter timing control for each exposure. This process runs in the background providing interaction with the hardware, from anywhere on the network, via a set of Python Remote Procedure Calls (RPC). The expose call is used to initiate an exposure, specifying the duration, binning, type (cal,zro,drk,etc) and a unique identifier for the exposure. Upon receipt of the expose command, CAMRA initiates an exposure with the underlying hardware controllers, then opens and closes the LCU shutter for the requested duration, then initiates the readout. Once the readout completes, data are copied from the individual amplifier image buffers to the corresponding FITS files.[11]

4. CHARACTERIZATION DATA SET

A suite of Python scrips that interact both with VDAS and the LCU were developed to automate the data taking process. Coordination of data taking with the turning on and off and shuttering in the LCU, two entirely separate systems, was necessary to ensure a stable setup for characterization. With 78 units to characterize, some automation of the characterization process is essential for efficiency. These scripts coordinate and control timing for the LDLS and instrument shutters, the status of the neutral density filter, and the turning on and off of lamps with VDAS exposure commands. User friendly Python functions allow the user to easily script the taking of custom data sets while writing proper data type values to headers and without worry of timing issues or hardware misuse. The suite also contains scripts for automated data taking of common data sets to characterization along with an automated routine for taking the entire characterization set. Table 1 lists the the data included in the characterization data set and its purpose (to be discussed in Sec. 5).

Table 1. This table shows data included in the characterization data set and a brief summary of its use.

Data Type	**Number of Images**	**Data Use**
Bias set value ramp	30 zeros with variable set values	Setting bias level (sec 5.1)
Bias set	31 zeros	Calculate read noise (sec 5.4)
Long darks	3 15 minute darks	Check for charge transfer
Pixel flat data (20,000DN)	31 flats and darks	Pixel flats (sec 5.2)
Pixel flat data (40,000DN)	15 flats and darks	Bad pixel masks (sec 5.5)
Photon transfer curve set	27 x 2 flat variable exp. times	Measure gain (sec 5.4)
Fiber flats	11 fiber images	Relative fiber throughput (sec 5.6)
Fiber arcs	11 fiber arcs	Measure wavelength solution
Masked fiber data	5 masked flats and arcs	Fiber profiles

5. CHARACTERIZATION OF EACH UNIT

Before the deployment of a VIRUS unit there are many stages of tests in order to properly characterize the system's performance and prepare the unit for science operation. The characterization setup and data set remain stable and consistent for each unit so statistical variations in performance can be evaluated and calibration data for later science reduction of data can be trusted. This section outlines procedures in characterization of a VIRUS unit that either evaluate its performance or prepare it for science operation before deployment.

It should be noted that an assessment of image quality and contrast is done as part of the alignment process. A camera must meet specification for image quality and contrast to be considered aligned and move on to

characterization. As a result, analysis of these parameters is not a part of performance evaluation for characterization as each unit has already been shown to meet the specification. For a detailed discussion of the alignment procedures and image quality testing refer to Ref. 7, 12.

5.1 Setting Bias Levels

VDAS allows the bias levels to be set by providing the controller with a set value number that corresponds to a voltage that sets the bias level. The bias levels that these set points correspond to are different for each controller requiring an analysis of the set value trend for each spectrograph unit before bias levels can be set for characterization.

There is a threshold voltage at which the bias will have a value, at which point the bias level increases non-linearly with the set value or voltage. At a high enough set value the relationship becomes linear. The bias levels for each chip are chosen to be in this linear regime and also have enough signal to properly sample any bias structure. Analysis of biases with different set values is required to find the set values for a corresponding biases level for each chip.

A set of bias is taken with increasing set values. Set values are plotted against averaged frame bias levels for each amplifier. A rough second derivative of the curve is calculated to find the linear region. Interpolation over the isolated linear region provides very accurate mapping between the set values and the corresponding bias levels. Figure 6 shows an example of the output plot of this analysis script. We chose to set the bias level at 1000 for all detectors because it falls well into the linear regime for the all CCDs. This also provides a high enough level to expose any potential bias structure while not sacrificing too much dynamic range.

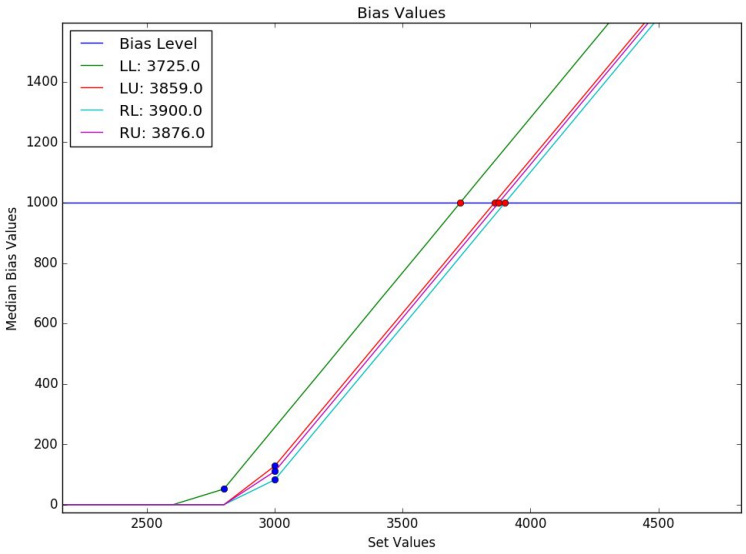

Figure 6. This plot shows the bias set values varied among a set of 50 bias images plotted against the bias values of the images for a single VIRUS unit (2 CCDs). The blue horizontal line shows the user desired bias level (we chose 1000). The blue points show where the code determines where the curve for each amplifier becomes linear. All data points above the blue points is interpolated over to find the set values corresponding to the chosen bias level. These are plotted in red. The set values are printed in the legend for each amplifier.

A python script automating this testing has been added to the data taking suite of scripts discussed in Sec. 4. This script contains a function for taking the set of ramped biases, a function for analyzing this data to find the set values for a user specified bias level, and a final function to set the biases for each amplifier. The values set by this script only temporarily store the values until the controller is reset. Configuration files for each unit are made that store the set values along with other information corresponding to the unit (eg. ID, gain, read

noise). VDAS loads the corresponding configuration file with each start of the camera server so bias levels are automatically set and spectrograph specific information is written to the data headers.

5.2 Pixel flats

The pixel flat data set includes 31 flat images of the same exposure level (20,000 DN) with corresponding darks. Scripts were written to perform a statistical check for drift in the average values (sometimes due to LDLS warmup) of the flats taken to be combined. This has allowed us to set a long enough warmup time in the data taking scripts for this to no longer be a concern. If the average of the flats checks out to be consistent, darks are subtracted and the resulting flat frames are combined into a master flat. Pixel flat images are made of each amplifier using scripts implementing CURE routines. CURE is the data reduction pipeline being written for the HETDEX survey.

The resulting pixel flat image is essentially the flat image where small QE pixel variations are eliminated. Pixels flats reveals structure or features in the detector that can not be eliminated through flat fielding. Refer to Fig. 7 for an example pixel flat of 4 amplifiers for a single unit. Pixel flats generated during characterization are needed for data reduction to divide out this structure from science and calibration images.

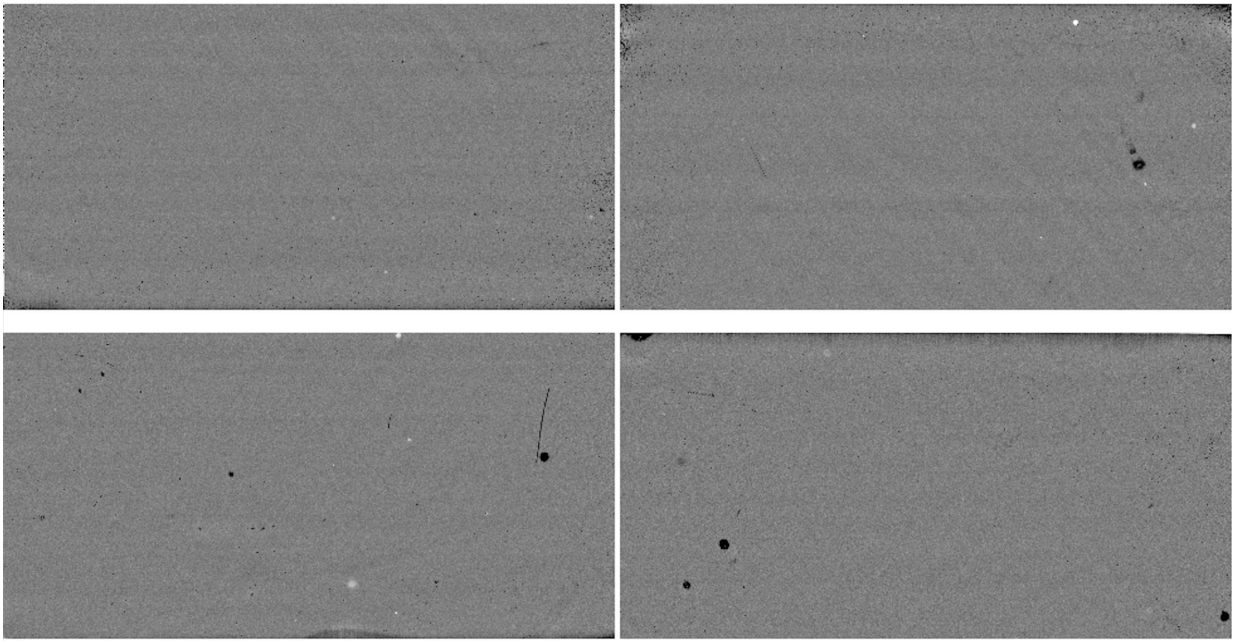

Figure 7. This is an example of a pixel flat generated for the four amplifiers of camera 37

Through examination of pixels flats it was found that the CCDs are highly susceptible to contamination causing features in the edges of the chip where the pixels had a much lower quantum efficiency. Tests are ongoing to determine the source of this contamination and if the detectors and/or cameras can be cleaned to reduce these features. Once this issue was discovered pixels flats were made for nearly all aligned cameras to use as a diagnostic for determining which cameras were ready for characterization before deployment. Units with the least prominent features were chosen for the first batch of deployed units and proceeded through characterization.

5.3 Read Noise

Read noise values were derived with a set of 31 biases. These bias images were stacked and a standard deviation was taken of each pixel. These standard deviation are plotted on a histogram and pixels outside of four sigma are masked. The average of of these standard deviations gives the read noise. We get an average read noise value of 3.19 electrons which is within the specification provided to the vendor.

5.4 Gain Measurements

Values for the gain are derived via the photon transfer method. Increasing signal values are plotted against variance (representing the total noise). The total noise curve is comprised of three regimes each representing a noise source of the system. The total noise of the detector is represented by

$$\sigma_{TOTAL} = (\sigma^2{}_{FP} + \sigma^2{}_{SHOT} + \sigma^2{}_{READ})^{1/2}. \quad (1)$$

Fixed pattern noise σ_{FP} comes from differences in pixel sensitivity across the chip. Some pixels will collect light more efficiently than others causing a fixed pattern of noise across the chip that increases linearly with signal. Because this noise is fixed it can easily be removed by subtracting consecutive images of the same exposure level and dividing by $\sqrt{2}$. Fixed pattern noise dominates the high signal end of the and once subtracted shot noise limit is reached.

Shot noise σ_{SHOT} involves how photons spatially arrive on the detector and can be described by Poisson statistics. ADC gain ($K_{ADC}(e-/DN)$) can be derived from the shot noise curve as it has the following dependence,

$$\sigma_{shot} = (\frac{S(DN)}{K_{ADC}(e-/DN)})^{1/2}., \quad (2)$$

Read noise is the remaining source of noise and has no signal dependence. It is the first regime and flat slope of the photon transfer curve. As the detector is illuminated the ptc moves into the shot noise regime with a slope of 1/2 dependence (in log log space) on the signal. At the high signal end the noise becomes dominated by fixed pattern noise as it increases linearly with signal. Fixed pattern noise exists as the slope 1 regime of the photon transfer curve.[13]

The photon transfer curve data set is taken as part of the full characterization set for each spectrograph unit. A series of flats are taken with the continuum LDLS source and pixel flat head with logarithmically increasing exposure times. Two sets of exposures are taken, utilizing two LCU modes, to efficiently sample the entire dynamic range of the detector (from the read noise regime to full well) . Due to the LCU being extremely efficient, a neutral density filter with an optical density of 4.0 is inserted to attempt to reach the read noise regime at the shortest exposure the LDLS shutter will allow (0.2 seconds). Fifteen exposures are taken with the neutral density filter to sample the low signal end. The high signal end of the spectrum is sampled with twelve exposures without the neutral density filter to decrease exposure time and take data set as efficiently as possible. This data set provides 27 points on the photon transfer curve from just above the read noise regime to about two points beyond full well.

PTC analysis is performed on only a region of the chip to exclude the edges. An average of the overscan region of each chip is first subtracted from the signal values. The average and standard deviation of the signal values of each chip are plotted against each other on a log-log scale to make the photon transfer curve. Consecutive images of the same exposure level are subtracted to calculate the fixed pattern noise and pattern strength. The shot noise curve can then be found by removing the fixed pattern noise and the read noise. Non-linearity of the shot noise curve is checked by making sure the shot noise curve has a 1/2 slope. Values for the gain can then be derived from the equation 2 above.

PTC analysis of fifteen VIRUS units proved some variability in signal level across the chip in the flat images likely due to slight differences in LDLS output across the spectral range being exposed via the grating. We dealt with the problem by breaking up the flat images into 100 pixel wide columns. These different regions of the chip are then plotted by their proper signal level on the PTC. Fig 9 shows the resulting PTC of camera 20 where the flats were broken up into 100 pixel wide columns.It appears the method of breaking up the images into columns better constrains the shot noise curve and thus the gain.

With two separately written codes employing this same fundamental method we found the gain values derived depend on how well we divide the image into similar exposure level regions. The gain values derived from these codes agree to within 4 percent. Gains of a few spectrographs will be derived with an Fe55 source to improve the

accuracy of these measurements. The Fe55 setup requires partial deconstruction of a spectrograph so the source can be mounted directly in front of the detector. Because this process is time consuming, these measurements will only be made with a few cameras. We will constrain the PTC procedure with these measurements allowing for automated gain measures during characterization for the rest of the units.

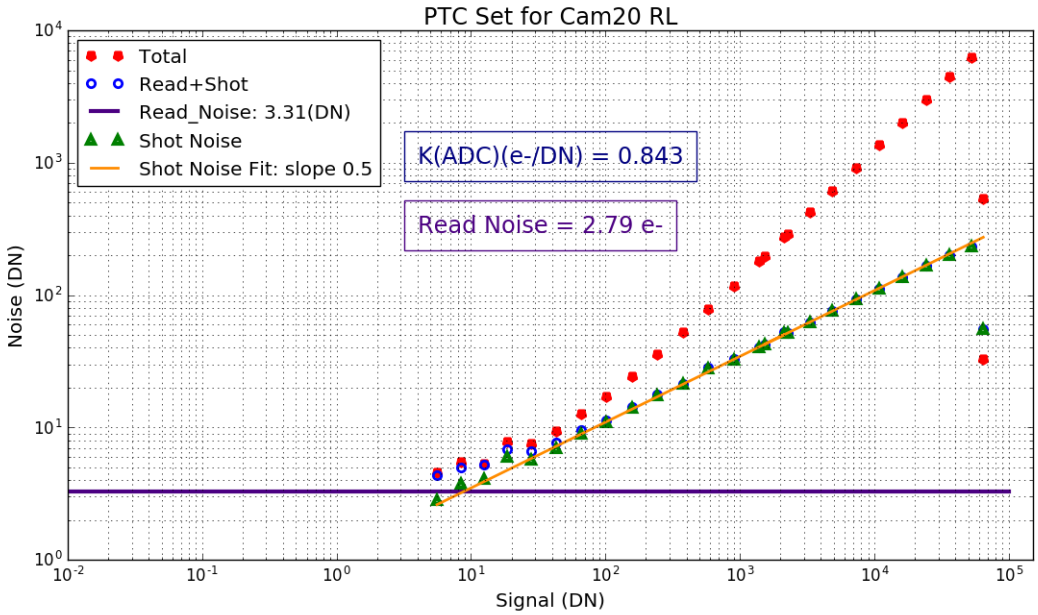

Figure 8. This is a plot of the PTC for camera 20 amplifier RL. Each point represents the value for the 27 images in the data set.

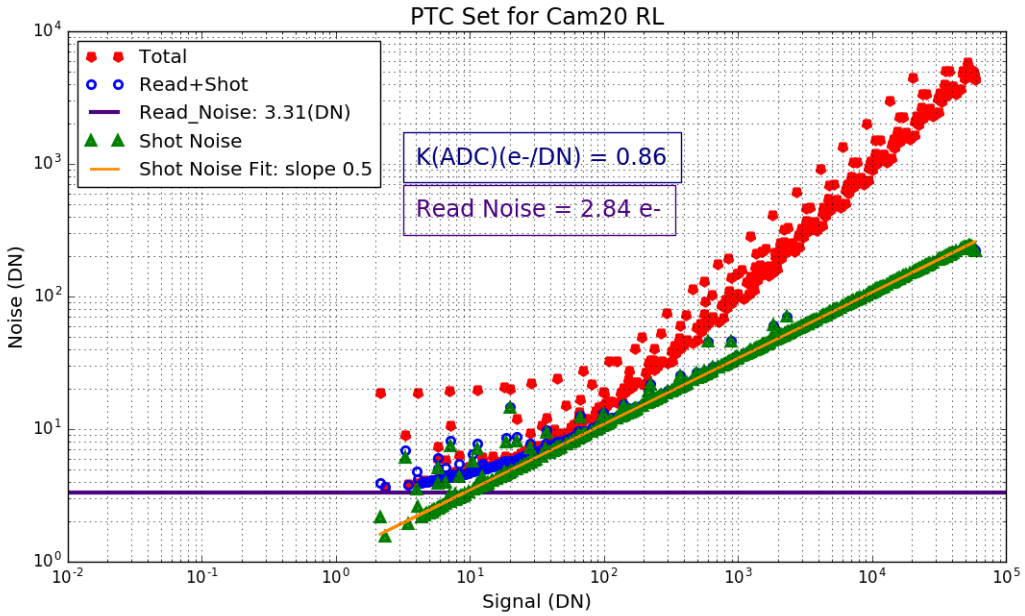

Figure 9. This is the PTC derived for camera 20 RL where a point is plotted for every 100 pixel wide column in the 27 images.

5.5 Bad pixel masks

Every CCD will have a few pixels that respond non-linearly and must be masked out of science data. A set of long exposure flats and short exposure flats (these short exposure flats are also used to make the pixel flats) are taken. An average of their corresponding dark frames are subtracted from each. An average high signal and low signal dark subtracted flat are made and then divided. This divided frame is normalized by the median frame value. Pixels with values greater than 1.5 times higher or 70 percent lower are flagged as bad pixels. A binary array of the CCD is made flagging the non-linearly responding pixels as zeros. This mask is used in the data reduction of this camera to mask out bad pixels.

5.6 Relative fiber throughput

A measure of the relative throughput from lab data is made to characterize a units performance. The same fiber bundle is used to take fiber flat and arcs during characterization of each unit. The lab setup and exposure times for each data set taken during characterization remain the same for every unit. Fiber flats and arcs are run through CURE (software being written to reduce and analyze VIRUS data) reduction routines to extract the spectrum for each fiber imaged on the detector. This reduction routine involves building averaged fiber flat and arc frames from overscan trimmed and bias subtracted images. CURE's deformer routine finds fiber traces from flats and builds a wavelength solution from tracing lines in arc frames. The distortion solution output from deformer gets fed into a CURE routine to extract the fibers. The integrated light of each spectrum is mapped back on to the fiber array. Relative throughput of each camera is then assessed by normalizing each fiber by the average of that fiber in all of the units fields. Essentially each field is normalized by the average of all of the fields. Normalizing the fields in this way removes fiber to fiber variations from the resulting array revealing how each unit performs relative to the others. The standard deviation of the averages of the frames is 0.067.

Similar analysis was performed on twilight flats taken on sky after the units were deployed to the HET. These twilight flats and arcs taken with the Facility Calibration Unit (FCU) of each camera were run through the same CURE reduction routine as the lab fiber data. Spectra from the fibers were summed and mapped onto their fields in the same way as shown in figure 11. All of the fibers in the fifteen fields are normalized by the average of all of the fibers in all of the fields. Sky data needed to be normalized differently from sky data because on the HET each unit is paired with its fiber bundle. As a result, fiber to fiber variation is not taken out of this data. Work is being done to remove the fiber variation measured at AIP of each fiber bundle from this data so that it can be more directly compared to lab data. The standard deviation of the averages of each frame in the sky data is 0.083.

To better evaluate performance of the units on sky, absolute throughput measurements must be made and this remains a goal of commissioning. Before proper absolute throughput measurements can be made, better modeling of telescope obstructions (eg. wide field corrector, track, fiber bundles) are necessary to understand the amount of light the telescopes sees as function of tracker position. Work is also being done to refine the fiber profiles of VIRUS units to ensure the right amount of light is extracted with each spectra for CURE reduction of the on sky data. Fiber profiles not being well constrained is not an issue for relative measurements discusses above but are essential for absolute measures of throughput.

6. VIRUS DEPLOYMENT TO THE HET

At this time fifteen units have gone through characterization at UT Austin and have been deployed to the HET. The units have been successfully installed in their enclosures and commissioning of the units has begun and remains ongoing. For a more detailed discussion about installation and commissioning of VIURS units refer to Ref. 14. For discussion on fiber bundle commissioning refer to Ref. 15.

7. SUMMARY OF CHARACTERIZATION OF THE FIRST FIFTEEN UNITS

We currently have a stable lab setup and nearly automated data taking routine for characterization. With the development of the final stage a VIRUS unit can be produced, assembled, and characterized cost effectively and efficiently in a semi-automated 'assembly line' fashion. Characterization of the first batch of eight VIRUS units

tested the automated data taking setup and proved its proficiency. After a camera is cooled the entire data set takes about 5 hours to complete but requires on average only about 30 minutes of the data takers time.

These first eight data sets have allowed us to develop and refine analysis procedures for the characterization of a unit. A summary and discussion of results of the first batch of characterized units is listed below:

1. We are able to successfully set the bias levels of each amplifier and store set values in the configuration file for each unit.
2. Pixel flats of each amplifier show the amount of pixels with low QE possibly as a result of contamination. Assessment of pixel flats allowed for the cleanest cameras to be selected for the first batch of deployment.
3. Read noise values are measured from a set of bias levels. The average read noise of this batch is 3.19 meeting specification supplied to the vendor.
4. Photon transfer curves are made to derive gain values. Due to wavelength dependent structure in the LDLS continuum source it was decided that an Fe55 source measurement is needed to add a known point to the ptc to better constrain our gain measurements.
5. Bad pixel masks are made for each detector and are delivered with each unit.
6. Relative performance of each unit are evaluated through relative throughput measures of each units field taken in lab and on sky. The standard deviations of relative throughput of the 15 units is 0.067 in lab and 0.083 on sky. The higher on sky standard deviation is probably mostly due to the fiber to fiber variability present in on sky data.

The 15 units chosen for deployment show small to no contamination when assessing their pixel flats. However, as we are now investing the source of contamination and the nature of the detectors susceptibility, we are unsure if it changes with time. As a precaution our plan for the 15 deployed cameras is for them to be replaced with clean cameras once they are ready. These units will return to UT-Austin to be cleaned in the same way, run through characterization, and redeployed. Deploying these 15 units before cleaning, however, was essential for the following reasons:

1. It allowed for testing of the infrastructure that houses and operates VIRUS on the HET.
2. We were able to begin commissioning of the wide field corrector upgrade on the HET.
3. Methods of installation of VIRUS units and fiber bundles on the HET were developed.
4. This early commissioning provided on sky data of a VIRUS unit necessary for development of CURE (the data reduction pipeline for VIRUS and the HETDEX survey)
5. Early commissioning also provided training for HET's telescope operators and resident astronomers on VIRUS observations before full science operation.
6. Running these units through characterization allowed us to constrain the data set and analysis needed of each unit before deployment

ACKNOWLEDGMENTS

HETDEX is run by the University of Texas at Austin McDonald Observatory and Department of Astronomy with participation from the Ludwig-Maximilians-Universitt Mnchen, Max-Planck-Institut fr Extraterrestriche-Physik (MPE), Leibniz-Institut fr Astrophysik Potsdam (AIP), Texas AM University, Pennsylvania State University, Institut fr Astrophysik Gttingen, University of Oxford and Max-Planck-Institut fr Astrophysik (MPA). In addition to Institutional support, HETDEX is funded by the National Science Foundation (grant AST-0926815), the State of Texas, the US Air Force (AFRL FA9451-04-2-0355), by the Texas Norman Hackerman Advanced Research Program under grants 003658-0005-2006 and 003658-0295-2007, and by generous support from private individuals and foundations.

We thank the staffs of McDonald Observatory, AIP, MPE, TAMU, Oxford University Department of Physics, and IAG for their contributions to the development of VIRUS. I would like to acknowledge Greg Ziemann for providing a Python wrapper that helped automate CURE reduction of the fiber data for relative throughput measurements. I would also like to thank members of the VIRUS undergraduate team, specifically Ingrid Johnson, Erasmo Azael Gonzalez, and Logan Pearce, for setup up and aiding in the data taking efforts.

REFERENCES

[1] Hill, G. J., Tuttle, S. E., Drory, N., Lee, H., Vattiat, B. L., DePoy, D. L., Marshall, J. L., Kelz, A., Haynes, D., Fabricius, M. H., Gebhardt, K., Allen, R. D., Anwad, H., Bender, R., Blanc, G., Chonis, T., Cornell, M. E., Dalton, G., Good, J., Jahn, T., Kriel, H., Landriau, M., MacQueen, P. J., Murphy, J. D., Peterson, T. W., Prochaska, T., Nicklas, H., Ramsey, J., Roth, M. M., Savage, R. D., and Snigula, J., "VIRUS: production and deployment of a massively replicated fiber integral field spectrograph for the upgraded Hobby-Eberly Telescope," *Proc. SPIE* **9147**, 27 (2014).

[2] Hill, G. J., Tuttle, S. E., Vattiat, B. L., Drory, N., Kelz, A., Ramsey, J., DePoy, D. L., Marshall, J. L., Gebhardt, K., Chonis, T., Dalton, G., Farrow, D., Good, J., Haynes, D., Indahl, B., Jahn, T., Kriel, H., Montesano, F., Nicklas, H., Noyola, E., Prochaska, T., Allen, R. D., Blanc, G., Fabricius, M. H., Landriau, M., MacQueen, P. J., Roth, M. M., Savage, R. D., and Snigula, J., "VIRUS: first deployment of the massively replicated fiber integral field spectrograph for the upgraded Hobby-Eberly Telescope," *Proc. SPIE* **9908**(54) (2016).

[3] Hill, G. J., Drory, N., Good, J., Lee, H., Vattiat, B. L., Kriel, H., Ramsey, J., Randy Bryant, R., Elliott, L., Fowler, J., Landriau, M., Leck, R., Odewahn, S., Perry, D., Savage, R., Schroeder Mrozinski, E., Shetrone, M., Damm, G., Gebhardt, K., MacQueen, P., Martin, J., Armandroff, T., and Ramsey, L., "The Hobby-Eberly Telescope wide-field upgrade," *Proc. SPIE* **9906**(5) (2016).

[4] Lee, H., Hill, G. J., Good, J., Vattiat, B., Shetrone, M., Martin, J., Schroeder Mrozinski, E., Kriel, H., Oh, C.-J., Frater, E., Smith, B., and Burge, J., "Delivery, installation, on-sky verification of Hobby Eberly Telescope wide-field corrector," *Proc. SPIE* **9906**(156) (2016).

[5] Adams, J. J., Blanc, G. A., Hill, G. J., Gebhardt, K., Drory, N., Hao, L., Bender, R., Byun, J., Ciardullo, R., Cornell, M. E., Finkelstein, S. L., Fry, A., Gawiser, E., Gronwall, C., Hopp, U., Jeong, D., Kelz, A., Kelzenberg, R., Komatsu, E., MacQueen, P. J., Murphy, J., Odoms, P. S., Roth, M., Schneider, D. P., Tufts, J. R., and Wilkinson, C. P., "The HETDEX Pilot Survey. I. Survey Design, Performance, and Catalog of Emission-line Galaxies," *ApJS* **192**, 5 (2011).

[6] Hill, G. J., MacQueen, P. J., Smith, M. P., Tufts, J. R., Roth, M. M., Kelz, A., Adams, J. J., Drory, N., Grupp, F., Barnes, S. I., Blanc, G. A., Murphy, J. D., Altmann, W., Wesley, G. L., Segura, P. R., Good, J. M., Booth, J. A., Bauer, S.-M., Popow, E., Goertz, J. A., Edmonston, R. D., and Wilkinson, C. P., "Design, construction, and performance of virus-p: the prototype of a highly replicated integral-field spectrograph for het," *Proc. SPIE* **7014**, 15 (2008).

[7] Tuttle, S. E., Hill, G. J., Lee, H., Vattiat, B., Noyola, E., Drory, N., Cornell, M., Peterson, T., Chonis, T., Allen, R., Dalton, G., DePoy, D., Edmonston, D., Fabricius, M., Haynes, D., Kelz, A., Landriau, M., Lesser, M., Leach, B., Marshall, J., Murphy, J., Perry, D., Prochaska, T., Ramsey, J., and Savage, R., "The construction, alignment, and installation of the virus spectrograph," *Proc. SPIE* **9147**, 13 (2014).

[8] Lesser, M., "Recent astronomical detector development at the university of arizona," *Proc. SPIE* **8453**, 14 (2012).

[9] Smith, M. P., Mulholland, G. T., Booth, J. A., Good, J. M., Hill, G. J., MacQueen, P. J., Rafal, M. D., Savage, R. D., and Vattiat, B. L., "The cryogenic system for the virus array of spectrographs on the hobby-eberly telescope," *Proc. SPIE* **7018**, 9 (2008).

[10] Chonis, T., "Using the VIRUS Lab Calibration Unit," (2016).

[11] Ramsey, J., Drory, N., Bryant, R., Elliott, L., Fowler, J., Hill, G. J., Landriau, M., Leck, R., and Vattiat, B. L., "A control system framework for the Hobby-Eberly Telescope," *Proc. SPIE* **9913**(160) (2016).

[12] Lee, H. and Hill, G. J., "Image moment-based wavefront sensing for in-situ full-field image quality assessment," *Proc. SPIE* **8450**, 14 (2012).

[13] Janesick, J. R., [*Photon Transfer DN* λ], SPIE (2007).

[14] Tuttle, S. E., Hill, G. J., Vattiat, B. L., Lee, H., Drory, N., Kelz, A., Ramsey, J., Peterson, T., Noyola, E., DePoy, D. L., Marshall, J. L., Chonis, T., Dalton, G., Fabricius, M. H., Farrow, D., Good, J., Haynes, D., Indahl, B., , Jahn, T., Kriel, H., Nicklas, H., Montesano, F., Prochaska, T., Allen, R. D., Landriau, M., MacQueen, P. J., Roth, M. M., Savage, R. D., and Snigula, J., "VIRUS early installation and commissioning.," *Proc. SPIE* **9908**(55) (2016).

[15] Kelz, A., Jahn, T., Hill, G. J., Tuttle, S. E., Vattiat, B. L., and Bauer, S. M., "Commissioning of VIRUS integral-field units at the Hobby-Eberly Telescope," *Proc. SPIE* **9908**(319) (2016).

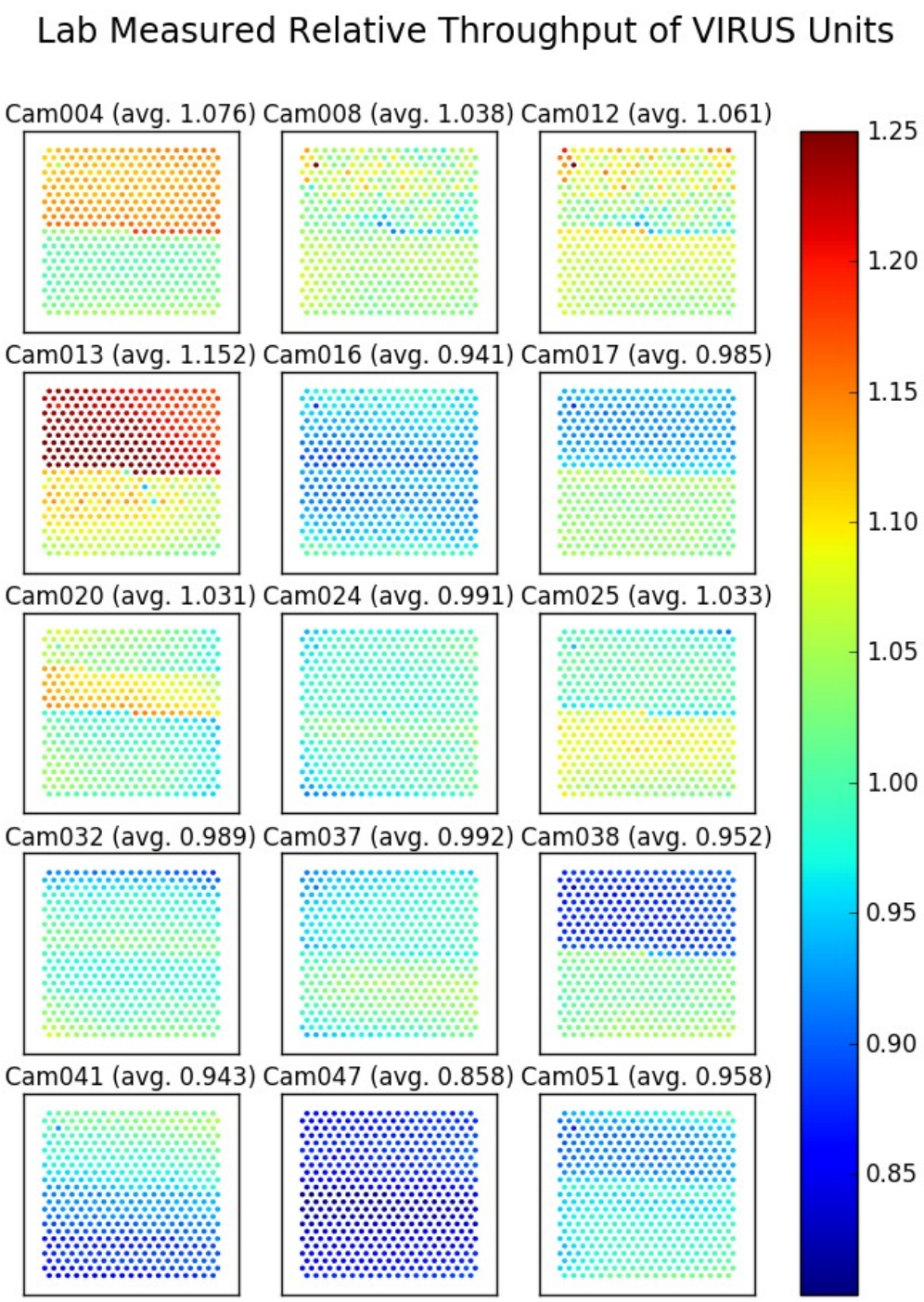

Figure 10. These plots show each of the fifteen deployed unit's summed spectra from lab data mapped back on to their field. Each field is normalized to the average of all of the fields removing fiber to fiber variations. This could be done because this data was taken for each unit with the same fiber bundle in lab as part of characterization. This plot represents relative throughput measures of each of the units providing a means to characterize their relative performance. The average of all the frames fibers are printed above each frame. The standard deviation of these values for all 15 frames is 0.067.

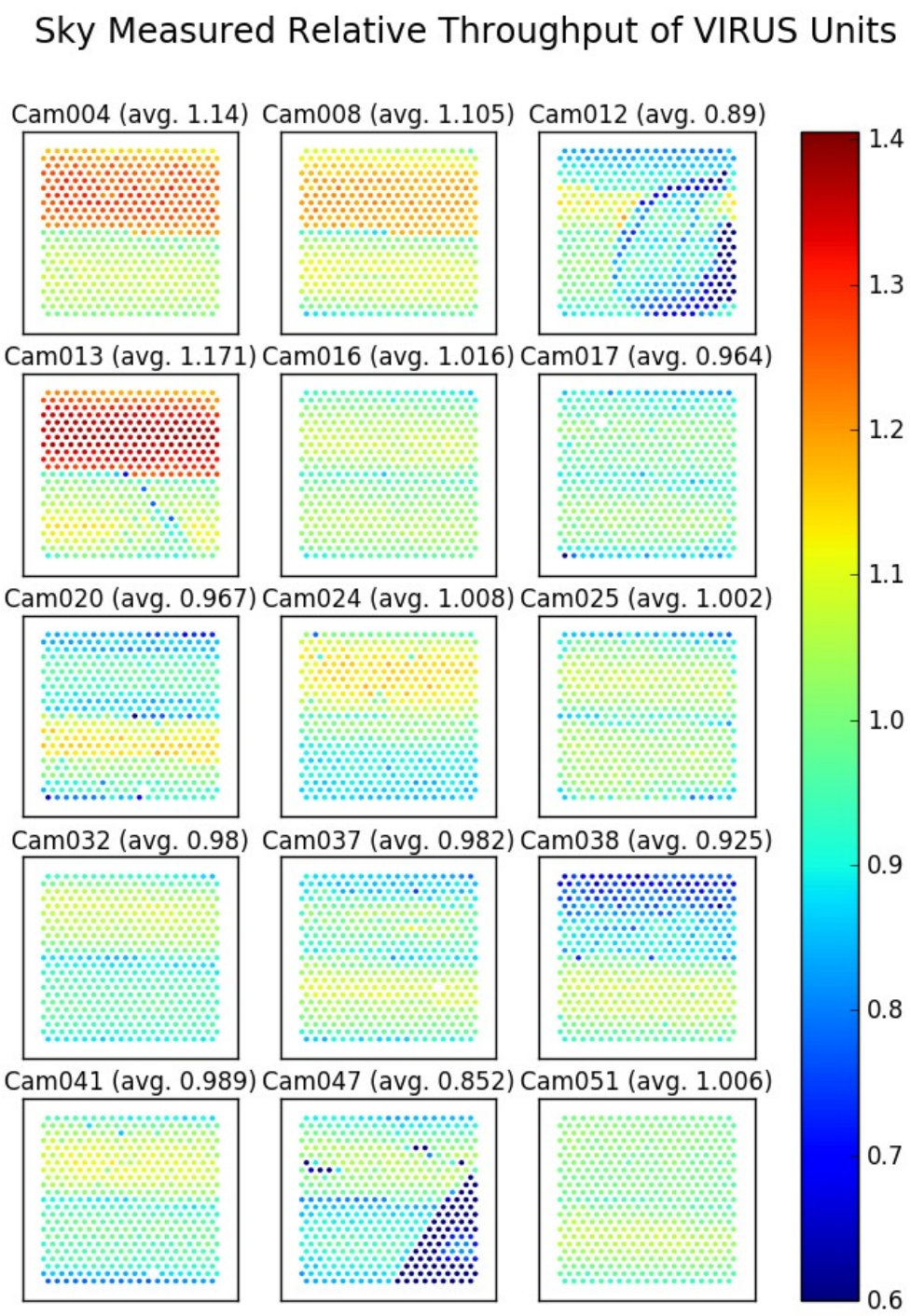

Figure 11. These plots show each of the fifteen deployed unit's summed spectra from twilight flats taken on sky mapped back on to their field. Each field is normalized by the average of all of the fibers in all of the fields. Sky frames were normalized differently from lab data because units are paired with their fiber bundles on the HET. As a result fiber to fiber variations could not be eliminated in these sky frames. The average of all the frames fibers are printed above each frame. The standard deviation of these values for all 15 frames is 0.083. The higher standard deviation seen on sky is probably mostly due to the fiber to fiber variation still present. Note that the low throughput regions in cameras 12 and 47 are due to cracked lenses on those fiber bundles.